

Property of Zero-energy Flows and Creations and Annihilations of Vortices in Quantum Mechanics

Tsunehiro Kobayashi*

*Department of General Education for the Hearing Impaired, Tsukuba College of Technology
Ibaraki 305-0005, Japan*

Abstract

Time-dependent processes accompanied by vortex creations and annihilations are investigated in terms of the eigenstates in conjugate spaces of Gel'fand triplets in 2-dimensions. Creations and annihilations of vortices are described by the insertions of unstable eigenstates with complex-energy eigenvalues into stable states written by the superposition of eigenstates with zero-energy eigenvalues. Some concrete examples are presented in terms of the eigenfunctions of the 2-dimensional parabolic potential barrier, i.e., $-m\gamma^2(x^2+y^2)/2$. We show that the processes accompanied by vortex creations and annihilations can be analyzed in terms of the eigenfunctions in the conjugate spaces of Gel'fand triplets. Throughout these examinations we point out three interesting properties of the zero-energy flows. (i) Mechanisms using the zero-energy flows are absolutely economical from the viewpoint of energy consumption. (ii) An enormous amount of information can be discriminated in terms of the infinite topological variety of the zero-energy flows. (iii) The zero-energy flow patterns are absolutely stable in any disturbance by inserting arbitrary decaying flows with complex-energy eigenvalues.

Keywords: Zero-energy solutions, vortex creations and annihilations, quantum mechanics, Gel'fand triplets,

*E-mail: kobayash@a.tsukuba-tech.ac.jp

1 Introduction

Vortices play interesting roles in various aspects of present-day physics such as vortex matters (vortex lattices) in condensed matters [1, 2], quantum Hall effects [3-7], various vortex patterns of non-neutral plasma [8-11] and Bose-Einstein gases [12-16]. In hydrodynamics the vortices are well known objects and has been investigated in many aspects [17-21]. A hydrodynamical approach was also vigorously investigated in the early stage of the development of quantum mechanics [22-29], and some fundamental properties of vortices in quantum mechanics were extensively examined by many authors [30-37].

Recently we have proposed a way to investigate vortex patterns in terms of zero-energy solutions of Schrödinger equations in 2-dimensions, which are eigenfunctions in conjugate spaces of Gel'fand triplets (CSGT) and degenerate infinitely [38, 39]. It should be noted that the eigenfunctions in CSGT represent scattering states, and thus they are generally not normalizable [40]. Therefore, the probability density ($|\psi|^2$) and the probability current ($\mathbf{j} = \text{Re}[\psi^*(-i\hbar\nabla)\psi]/m$) for the eigenfunction (ψ), which are defined in usual Hilbert spaces, cannot be introduced to the eigenfunctions in CSGT. Instead of the probability current, however, the velocity which is defined by $\mathbf{v} = \mathbf{j}/|\psi|^2$ can have a well-defined meaning, because the ambiguity due to the normalization of the eigenfunctions disappears in the definition of the velocity. Actually we have shown that many interesting objects used in hydrodynamics such as the complex velocity potential can be introduced in the 2-dimensions of CSGT [41]. We can expect that the hydrodynamical approach is a quite hopeful framework in the investigation of phenomena described in CSGT. One should pay attention to two important facts obtained in the early works [38,39]. One is the fact that the zero-energy solutions are common over the two-dimensional central potentials such that $V_a(\rho) = -a^2 g_a \rho^{2(a-1)}$ with $\rho = \sqrt{x^2 + y^2}$ except $a = 0$ and then similar vortex patters described by the zero-energy solutions appear in all such potentials. Actually zero-energy solutions for a definite number of a can be transformed to solutions for arbitrary number of a by conformal mappings [38, 39]. The other is that the zero-energy solutions are infinitely degenerate, and thus all energy eigenvalues in CSGT with the potentials $V_a(\rho)$ are infinitely degenerate because the addition of the infinitely degenerate zero-energy solutions to arbitrary eigenfunctions does not change the energy eigenvalues at all. It should also be pointed out that non-zero energy solutions in CSGT generally have complex energy eigenvalues like $\mathcal{E} = E \mp i\Gamma$ with $E, \Gamma \in \mathbb{R}$ and then their time developments are described by the factors $e^{-(iE/\hbar \pm \Gamma/\hbar)t}$ [40]. We see that stationary flows and time-dependent flows are, respectively, represented by the zero-energy solutions and the non-zero energy solutions in CSGT. From these facts it can be expected that in CSGT time-dependent flows in real processes are described by linear combinations of some stationary flows written by the zero-energy solutions and non-stationary flows (time-dependent flows) given by non-zero (complex) energy solutions. In such flows vortex patterns will become important objects to identify the situations of the flows. We can image two different types of the vortex patterns. One is the stationary vortex patterns, and the other is the vortex patterns changing in the time developments, which have been observed in real processes

associated with vortices [8-16]. As presented in our early works [38, 39], the stationary vortex patterns can be described by the superposition of the zero-energy solutions, while the time-dependent ones will be done by putting the non-zero energy solutions into the superposition. In this paper we shall study time-dependent vortex patterns accompanied by vortex creations and annihilations in terms of the eigenfunctions of 2D-PPB in CSGT, since the eigenfunctions with non-zero energy (complex energy) solutions in CSGT are known only in the case of the PPB. We shall also see that this approach can be one possibility to analyze various time-dependent vortex patterns in a rigorous framework of quantum mechanics in CSGT.

A brief review on the eigenfunctions of 2D-PPB [41] and also the vortices in the hydrodynamical approach of quantum mechanics is presented in the section 2. In the section 3 various vortex patterns accompanied by vortex creations and annihilations are investigated in terms of the eigenfunctions of the PPB given in the section 2. In the section 4 discussions on problems in this approach are performed and an application of this model to processes transmitting an enormous amount of information by a very small energy consumption and also preserving the information (making memories) stably as well is noticed.

2 Brief review on the eigenfunctions of 2D-PPB and vortices

2-1 Eigenfunctions of 2D-PPB

The infinitely degenerate eigenfunctions with the zero-energy for the potentials $V_a(\rho)$ have explicitly been given in the papers [38, 39], whereas the eigenfunctions with non-zero energies are known only in the case of parabolic potential barriers (PPB) [41-47]. In order to make some concrete examples of time-dependent vortex patterns we perform the following considerations in terms of eigenfunctions of a two-dimensional parabolic potential barrier (2D-PPB) $V = -m\gamma^2(x^2 + y^2)/2$, which are already obtained in the paper [41]. Here we shall summarize the results for the 2D-PPB, which will be used in the following discussions. It is trivial that the eigenfunctions in the 2D-PPB are represented by the multiples of those of the 1D-PPB as the eigenfunctions of 2D-harmonic oscillator (2D-HO) are done by those of the 1D-HO. The eigenfunctions of the 1D-PPB for x , which have pure imaginary energy eigenvalues $\mp i(n_x + \frac{1}{2})\hbar\gamma$, are given by

$$u_{n_x}^{\pm}(x) = e^{\pm i\beta^2 x^2/2} H_{n_x}^{\pm}(\beta x) \quad (\beta \equiv \sqrt{m\gamma/\hbar}), \quad (1)$$

where $H_{n_x}^{\pm}(\beta x)$ are the polynomials of degree n_x written in terms of Hermite polynomials $H_n(\xi)$ with $\xi = \beta x$ as [46, 47]

$$H_n^{\pm}(\xi) = e^{\pm i n \pi/4} H_n(e^{\mp i \pi/4} \xi). \quad (2)$$

We have four different types of the eigenfunctions in the 2D-PPB [41]. Two of them

$$U_{n_x n_y}^{\pm\pm}(x, y) \equiv u_{n_x}^{\pm}(x) u_{n_y}^{\pm}(y)$$

with the energy eigenvalues $\mathcal{E}_{n_x n_y}^{\pm\pm} = \mp i(n_x + n_y + 1)$, respectively, represent diverging and converging flows. (See figs. 1 and 2.) Some examples for the low degrees are obtained as follows;

$$\begin{aligned}
U_{00}^{\pm\pm}(x, y) &= e^{\pm i\beta^2(x^2+y^2)/2}, \\
U_{10}^{\pm\pm}(x, y) &= 2\beta x e^{\pm i\beta^2(x^2+y^2)/2}, \\
U_{01}^{\pm\pm}(x, y) &= 2\beta y e^{\pm i\beta^2(x^2+y^2)/2}, \\
U_{20}^{\pm\pm}(x, y) &= (4\beta^2 x^2 \mp 2i) e^{\pm i\beta^2(x^2+y^2)/2}, \\
U_{11}^{\pm\pm}(x, y) &= 4\beta^2 xy e^{\pm i\beta^2(x^2+y^2)/2}, \\
U_{02}^{\pm\pm}(x, y) &= (4\beta^2 y^2 \mp 2i) e^{\pm i\beta^2(x^2+y^2)/2}.
\end{aligned} \tag{3}$$

It is transparent that the eigenfunctions of angular momentums are constructed in terms of the linear combinations of these diverging and converging flows. Examples for some low angular momentums are presented in ref. [41]. The other two

$$U_{n_x n_y}^{\pm\mp}(x, y) \equiv u_{n_x}^{\pm}(x) u_{n_y}^{\mp}(y) \quad \text{with} \quad \mathcal{E}_{n_x n_y}^{\pm\mp}(x, y) = \mp i(n_x - n_y)$$

are corner flows round the center. (See figs. 3 and 4.) The zero-energy solutions that are common in the potentials $V_a(\rho)$ appear when $n_x = n_y$ is satisfied. A few examples of the zero-energy eigenfunctions are obtained as follows;

$$\begin{aligned}
U_{00}^{\pm\mp}(x, y) &= e^{\pm i\beta^2(x^2-y^2)/2}, \\
U_{11}^{\pm\mp}(x, y) &= 4\beta^2 xy e^{\pm i\beta^2(x^2-y^2)/2}, \\
U_{22}^{\pm\mp}(x, y) &= 4[4\beta^4 x^2 y^2 + 1 \pm 2i\beta^2(x^2 - y^2)] e^{\pm i\beta^2(x^2-y^2)/2}.
\end{aligned} \tag{4}$$

The existence of the infinitely degenerate zero-energy solutions brings the infinitely degeneracy to all the eigenstates with definite energies. This fact means that the energy and the other quantum numbers which are related to the determination of the energy eigenvalues like angular momentums are not enough to discriminate the eigenstates. What are the quantum numbers to characterize the infinite degeneracy? One interesting candidate to characterize the states is vortex patterns, which can be observable in experiments [8-16]. Time-dependences of the patterns are also good candidates for observables in those processes. It is obvious that the eigenfunctions of (13) and (14) are not normalizable. The details on the proof that they are the eigenfunctions of CSGT are presented in refs. [46,47].

2-2 Vortices in quantum mechanics

Let us here briefly note how vortices are interpreted in quantum mechanics. The probability density $\rho(t, x, y)$ and the probability current $\mathbf{j}(t, x, y)$ of a wavefunction $\psi(t, x, y)$ in non-relativistic quantum mechanics are defined by

$$\rho(t, x, y) \equiv |\psi(t, x, y)|^2, \tag{5}$$

$$\mathbf{j}(t, x, y) \equiv \text{Re} [\psi(t, x, y)^* (-i\hbar \nabla) \psi(t, x, y)] / m. \tag{6}$$

They satisfy the equation of continuity $\partial\rho/\partial t + \nabla \cdot \mathbf{j} = 0$. Following the analogue of the hydrodynamical approach [17-21], the fluid can be represented by the density ρ and the fluid velocity \mathbf{v} . They satisfy Euler's equation of continuity

$$\frac{\partial\rho}{\partial t} + \nabla \cdot (\rho\mathbf{v}) = 0. \quad (7)$$

Comparing this equation with the continuity equation, the following definition for the quantum velocity of the state $\psi(t, x, y)$ is led in the hydrodynamical approach;

$$\mathbf{v} \equiv \frac{\mathbf{j}(t, x, y)}{|\psi(t, x, y)|^2}. \quad (8)$$

Now it is obvious that vortices appear at the zero points of the density, that is, the nodal points of the wavefunction. At the vortices, of course, the current \mathbf{j} must not vanish. When we write the wavefunction $\psi(t, x, y) = \sqrt{\rho(x, y)}e^{iS(x, y)/\hbar}$, the velocity is given by $\mathbf{v} = \nabla S/m$. We should here remember that the solutions degenerate infinitely. This fact indicates that we can construct wavefunctions having the nodal points at arbitrary positions in terms of linear combinations of the infinitely degenerate solutions [38, 39, 41].

The strength of vortex is characterized by the circulation Γ that is represented by the integral round a closed contour C encircling the vortex such that

$$\Gamma = \oint_C \mathbf{v} \cdot d\mathbf{s} \quad (9)$$

and it is quantized as

$$\Gamma = 2\pi l\hbar/m, \quad (10)$$

where the circulation number l is an integer [31, 33, 35, 37].

3 Stationary vortex patterns and vortex creations and annihilations

Let us investigate vortex patterns in terms of the 2D-PPB eigenfunctions given in (3) and (4). Since the zero-energy solution given in (4) have no nodal point, they have no vortex. However, it has been shown that some vortex patterns having infinite numbers of vortices, like vortex lines and vortex lattices, can be made in terms of simple linear combinations of those low lying stationary states in the early works [38, 39]. We can, of course, make linear combinations having a few or some vortices. In the following discussions we shall study compositions not only for stationary vortex patterns but also for patterns accompanied by vortex creations and annihilations on the basis of a stationary flow having no vortex (we shall call it the basic flow hereafter). In these composition processes we shall see that various vortex patterns will be an understandable problem in quantum mechanics

by considering eigenstates in CSGT. As the basic flow without any vortices we take the flow described by

$$\begin{aligned}\Phi_B &= \frac{1}{4}U_{22}^{+-}(x, y) - U_{00}^{+-}(x, y) \\ &= (4\beta^4 x^2 y^2 + 2i\beta^2(x^2 - y^2))e^{i\beta^2(x^2 - y^2)/2}.\end{aligned}\quad (11)$$

Note that the nodal point at the origin does not produce vortices, because the current vanishes there.

3-1 Stationary vortex patterns

At first we shall show two stationary patterns with three and four vortices, which will be used in the following discussions on vortex creations and annihilations.

(1-1) Three vortices pattern

The linear combination of the basic flow and U_{22}^{+-} such that

$$\begin{aligned}\Phi_{012}^{+-}(x, y) &= \Phi_B - c^2 U_{11}^{+-}(x, y) \\ &= [4\beta^2 xy(\beta^2 xy - c^2) + 2i\beta^2(x^2 - y^2)]e^{i\beta^2(x^2 - y^2)/2},\end{aligned}\quad (12)$$

with $c \in \mathbb{R}$ has three vortices at the origin and the two points $(\pm c/\beta, \pm c/\beta)$ as shown in fig. 5. If we take $-c^2$ instead of c^2 , three vortices appear at the origin and the points $(\pm c/\beta, \mp c/\beta)$.

(1-2) Four vortices pattern

The linear combinations given by

$$\begin{aligned}\Phi_{02}^{+-}(x, y) &= \frac{1}{4}\Phi_B - c^4 U_{00}^{+-}(x, y) \\ &= [(\beta^2 xy - c^2)(\beta^2 xy + c^2) + i\beta^2(x^2 - y^2)/2]e^{i\beta^2(x^2 - y^2)/2},\end{aligned}\quad (13)$$

has four vortices at the points $(\pm c/\beta, \pm c/\beta)$ and $(\pm c/\beta, \mp c/\beta)$ as shown in fig. 6.

3-2 Time-dependent patterns accompanied by vortex creations and annihilations

Let us go to the study of time-dependent vortex patterns that are obtained by linear combinations of stationary flows and time dependent ones. We shall see some simple vortex creation and annihilation processes. In the following considerations the time dependent flows are put in the stationary flows at $t = 0$.

Let us first discuss the processes where some vortices are once created and then they are annihilated in the time development.

(2-1) A pattern accompanied by a pair creation and annihilation

Let us consider the following linear combination;

$$\begin{aligned}\Phi_{02,1}^{+-}(x, y, t) &= \frac{1}{2}\Phi_B - \theta(t)c^3 U_{10}^{+-}(x, y)e^{-\gamma t} \\ &= [2\beta x(\beta^3 xy^2 - \theta(t)c^3 e^{-\gamma t}) + i\beta^2(x^2 - y^2)]e^{i\beta^2(x^2 - y^2)/2},\end{aligned}\quad (14)$$

where the theta function is taken as $\theta(t) = 0$ for $t < 0$ and $= 1$ for $t \geq 0$. It has two nodal points at $(ce^{-\gamma t/3}/\beta, \pm ce^{-\gamma t/3}/\beta)$ for $t \geq 0$, where two vortices with opposite circulation numbers exist. The nodal points go to the origin as the time t goes to infinity as shown in fig. 7. Since the contribution of the unstable flow decreases as $t \rightarrow \infty$ because of the time factor $e^{-\gamma t}$, the wavefunction $\Phi_{02,1}^{+-}(x, y, t)$ goes to Φ_B as $t \rightarrow \infty$. Thus the flow has no nodal point in the limit. This means that the pair of vortices which are created at $t = 0$ disappears at origin in the limit $t \rightarrow \infty$. We can say that this wavefunction describes the pair annihilation of two vortices. The time development of this process can be described as follows:

- (i) Before the time-dependent flow is put in the basic flow, i.e., $t < 0$, there is no vortex.
- (ii) At $t = 0$ when the time-dependent flow is put in the basic flow, a pair of vortices are suddenly created.
- (iii) The pair moves toward the origin, and then they annihilate at the origin, that is, the flow turns back to the basic flow Φ_B having no vortex.

(2-2) A pattern accompanied by creations and annihilations of two pairs

The linear combination given by

$$\begin{aligned}\Phi_{02,2}^{+-}(x, y, t) &= \Phi_B - \theta(t)c^2[2iU_{00}^{+-}(x, y) - U_{20}^{+-}(x, y)e^{-2\gamma t}] \\ &= [4\beta^2x^2(\beta^2y^2 - \theta(t)c^2e^{-2\gamma t}) - 2i(\theta(t)c^2(1 - e^{-2\gamma t}) - \beta^2(x^2 - y^2))]e^{i\beta^2(x^2 - y^2)/2}\end{aligned}\quad (15)$$

has four nodal points at $(\pm c/\beta, ce^{-\gamma t}/\beta)$ and $(\pm c/\beta, -ce^{-\gamma t}/\beta)$ for $t \geq 0$. In this case we easily see that the pair of vortices at $(\pm c/\beta, ce^{-\gamma t}/\beta)$ and that at $(\pm c/\beta, -ce^{-\gamma t}/\beta)$ annihilate as $t \rightarrow \infty$ as shown in fig. 8. The stationary flow $\Phi_B - 2ic^2U_{00}^{+-}(x, y)$ that appears in the limit has two nodal points at $(\pm c/\beta, 0)$, but it has no vortex, because the current also vanishes at the points. The time development of this process is interpreted similarly as the case (1-1).

In these two cases all vortices move on straight lines in the pair annihilation processes.

(2-3) A pattern accompanied by creation and annihilation of four vortices

The linear combinations of stationary solutions and diverging or converging flows make different types of annihilation processes. For an example, let us consider the linear combination of Φ_B and the lowest order diverging flow described by

$$U_{00}^{++}(x, y, t) = e^{i\beta^2(x^2 + y^2)/2}e^{-\gamma t} \quad (16)$$

having the energy eigenvalue $-i\gamma\hbar$. Let us consider the linear combination described by

$$\begin{aligned}\Phi_{02,0}^{++}(x, y, t) &= \frac{1}{4}\Phi_B - \theta(t)c^2U_{00}^{++}(x, y, t) \\ &= [\beta^4x^2y^2 - \theta(t)c^2e^{-\gamma t}e^{i\beta^2y^2} + i\beta^2(x^2 - y^2)/2]e^{i\beta^2(x^2 - y^2)/2}.\end{aligned}\quad (17)$$

For $t \geq 0$ it has two nodal points at the points where the following relations are fulfilled;

$$XY = c(t)\cos Y, \quad \frac{1}{2}(X - Y) - c(t)\sin Y = 0, \quad (18)$$

where $X = \beta^2 x^2$, $Y = \beta^2 y^2$ and $c(t) = c^2 e^{-\gamma t}$. From these relations we have an equation for Y

$$Y^2 - c(t)\cos Y + 2c(t)Y\sin Y = 0. \quad (19)$$

The solutions are obtained from the cross points of two functions $f(Y) = Y^2$ and $g(Y) = c(t)(\cos Y - 2Y\sin Y)$. We easily see that a solution for $Y \geq 0$ exists in the region $0 < Y < \pi/2$ for arbitrary positive numbers of $c(t)$. Four vortices appear at the four points expressed by the combinations of $x = \pm\sqrt{X}/\beta$ and $y = \pm\sqrt{Y}/\beta$, where X is obtained by using the first relation of (18). Since $c(t)$ goes to 0 as $t \rightarrow \infty$, we see that X and Y simultaneously go to 0 in the limit such that

$$X \simeq Y \rightarrow |c|e^{-\gamma t/2} \rightarrow 0, \quad \text{for } t \rightarrow \infty.$$

Since the flow turns back to the basic flow, the four vortices annihilate at the origin in the limit. From the second relation of (18), we have

$$X = Y + 2c(t)\sin Y.$$

This equation show us that the vortex points do not move toward the origin along straight lines.

Here we consider two somewhat complicated processes.

(2-4) A pattern accompanied by a pair annihilation and creation

Let us start from the stationary flow described by the wavefunction $\Phi_{012}^{+-}(x, y)$ of (12), which has three vortices. We consider a linear combination of the stationary state and a time-dependent flow described by

$$\Psi_2^{+-}(x, y; t) = (U_{20}^{+-} + U_{02}^{+-})e^{-2\gamma t} \quad (20)$$

such that

$$\begin{aligned} \Phi_{012,2}^{+-}(x, y; t) &= \Phi_{012}^{+-}(x, y) + \theta(t)\frac{1}{2}ai\Psi_2^{+-}(x, y; t) \\ &= \{4\beta^2 xy(\beta^2 xy - c^2) + 2i[(1 + \theta(t)a(t))\beta^2 x^2 - (1 - \theta(t)a(t))\beta^2 y^2]\} e^{i\beta^2(x^2 - y^2)/2}, \end{aligned} \quad (21)$$

where $a \in \mathbb{R}$ and $a(t) = ae^{-2\gamma t}$. For $t \geq 0$ the nodal points of the wavefunction appear at the points fulfilled the following relations;

$$\xi\eta(\xi\eta - c^2) = 0, \quad (1 + a(t))\xi^2 - (1 - a(t))\eta^2 = 0, \quad (22)$$

where $\xi = \beta x$ and $\eta = \beta y$. We easily see that for $|a(t)| > 1$ the second relation has only one solution at $\xi = \eta = 0$, whereas for $|a(t)| < 1$ it has two non-zero solutions at

$$\xi(t) = \pm\left(\frac{1 - a(t)}{1 + a(t)}\right)^{1/4}c, \quad \eta(t) = \pm\left(\frac{1 + a(t)}{1 - a(t)}\right)^{1/4}c. \quad (23)$$

This means that at the critical time t_c satisfying the relation $|a(t_c)| = 1$, that is,

$$t_c = \frac{1}{\gamma} \ln|a| \quad (24)$$

a pair of vortices are suddenly created at the two points $(\xi(t_c)/\beta, \eta(t_c)/\beta)$. We can interpret this process for $|a| > 1$ as follows (see also figs. 9, 10, 11 and 12):

- (i) Before the shock described by the time-dependent flow $\Psi_2^{+-}(x, y; t)$ is given, the flow is described by the stationary flow $\Phi_{012}^{+-}(x, y)$ with three vortices given in fig. 9.
- (ii) At $t = 0$ the shock is given, and then two vortices at two points $(\pm c/\beta, \pm c/\beta)$ suddenly disappear. (See fig. 10.)
- (iii) At the critical time $t = t_c$ two vortices again suddenly appear at $(\xi(t_c)/\beta, \eta(t_c)/\beta)$, and they move toward the original positions $(\pm c/\beta, \pm c/\beta)$ for $t > t_c$. (See fig. 11.)
- (iv) Finally the flow turns back to the original stationary flow. (See fig. 12.)

Throughout this process the vortex being at the origin does not move at all.

(2-5) A pattern accompanied by eight vortices annihilation

Here we take $\Phi_{02}^{+-}(x, y)$ of (13) as the stationary flow, which has four vortices. For the simplicity $c = 1/2$ is taken in the following discussions. Here the lowest order diverging flow $U_{00}^{++}(x, y, t)$ are put into the stationary flow at $t = 0$. The wavefunction are given by

$$\begin{aligned} \Phi_{02,0}^{++}(x, y; t) &= 16\Phi_{02}^{+-}(x, y) + \theta(t)b^2U_{00}^{++}(x, y, t) \\ &= [16\beta^4x^2y^2 - 1 + \theta(t)b^2e^{-\gamma t}e^{i\beta^2y^2} + 8i\beta^2(x^2 - y^2)]e^{i\beta^2(x^2 - y^2)/2} \\ &= [16\beta^4x^2y^2 - 1 + \theta(t)b(t)e^{-\gamma t}\cos(\beta^2y^2) + i(8\beta^2(x^2 - y^2) \\ &\quad + \theta(t)b(t)e^{-\gamma t}\sin(\beta^2y^2))]e^{i\beta^2(x^2 - y^2)/2}, \end{aligned} \quad (25)$$

where $b \in \mathbb{R}$ and $b(t) = b^2e^{-\gamma t}$. Using $X = \beta^2x^2$ and $Y = \beta^2y^2$, we have two relations for nodal points of the wavefunction for $t > 0$ as follows;

$$16XY + b(t)\cos Y - 1 = 0, \quad 8(X - Y) + b(t)\sin Y = 0, \quad (26)$$

From these relations we obtain an equation for the nodal points

$$1 - b(t)\cos Y - 16Y^2 + 2b(t)Y\sin Y = 0. \quad (27)$$

Examining the cross point of the two functions $F(Y) = 16Y^2 - 1$ and $G(Y) = -b(t)(\cos Y - 2Y\sin Y)$, we obtain the following results:

- (1) In the case of $b(t) < 1$ the two functions always have a cross-point in the region satisfying $Y \geq 0$ (note that $Y = \beta^2y^2$). The wavefunction, therefore, has four nodal points. This means that the flow always has four vortices that move toward the stationary points fulfilling $|x| = |y| = (2\beta)^{-1}$ as t increases.
- (2) In the case of $b(t) > 1$ eq.(27) has an even number of solutions like $n = 0, 2, 4, \dots$. Since one solution brings four vortices on a circle with the center at the origin, the vortex number is given by $4n$. Note that the number n increases as $b(t)$ increases. This fact

means that, since $b(t)$ decreases as t increases, the vortex number decreases as t increases until $b(t)$ gets to 1. Considering that the change of n is always 2, we see that the reduction of the vortex number caused by the change of n is always 8. That is to say, we observe that four vortex-pairs simultaneously annihilate at four different points on a circle. As a simple example, let us consider the case of $n = 2$ at $t = 0$. We observe the following time development of the flow:

- (i) For $t < 0$ the stationary flow has the four vortices as shown in fig.6.
- (ii) At $t = 0$ the original four vortices disappear and eight vortices are newly created. Then we observe the flow having eight vortices. (See fig. 13.)
- (iii) In the time-development the eight vortices disappear simultaneously. We observe the process as the annihilations of four vortex-pairs. Thus the flow having no vortex appears.
- (iv) At the critical time $t_c = \ln b^2 / \gamma$ when $b(t_c) = 1$ is fulfilled four vortices are created at the origin, and then they move toward the stationary points. The vortex state at $t = t_c$ can be understood as a vortex quadrupole [38].

If, instead of the diverging flow $U_{00}^{++}(x, y, t)$, the converging flow $U_{00}^{--}(x, y, t)$ is put in the stationary flow, we observe a flow continuously creating 8 vortices for any choices of b . Of course, the time dependent flow blows up the magnitude in the limit of $t \rightarrow \infty$, and thus the original stationary flow can not be observed in the limit.

4 Discussions

We have shown concrete examples of different types of vortex patterns accompanied by creations and annihilations of vortices by using only some low degree solutions of the 2D-PPB. We can, of course, present more complicated patterns by introducing the higher degree solutions, but the examples presented in the section 3 will be enough to show the fact that various vortex patterns can be reproducible in terms of the eigenfunctions of the 2D-PPB. As already noted that the zero-energy solutions in the 2D-PPB can be transformed to those in the potentials $V_a(\rho)$ by the conformal mappings [38,39], the stationary patterns given in the section 3-1 can be mapped into the stationary patterns of arbitrary potentials. This fact means that, as far as the stationary patterns are concerned, there is an exact one-to-one correspondence between the patterns of the PPB and those of the other potentials. As for the time-dependent patterns we cannot present any concrete examples except the case of the 2D-PPB at this moment, but we may expect that similar vortex patterns as those given in the section 3-2 for the PPB will appear in other potentials, since all energy eigenstates with complex eigenvalues degenerate infinitely in all the potentials $V_a(\rho)$ as same as in the 2D-PPB. Anyhow we cannot exactly say about the problem before we find any solutions with complex eigenvalues in the other cases.

Here we would like to note 2D-PPB. We do not know any physical phenomena that are described by 2D-PPB. We can, however, expect that most of weak repulsive forces in matters composed of many constituents will be approximated by PPBs as most of weak attractive forces are well approximated by harmonic oscillators. In general flows that go

round a smooth hill of potential feel a weak repulsive force represented by a PPB [48-50]. Actually we see that when a charged particle is put in an infinitely long tube where same charged particles are uniformly distributed, the charged particle feels 2D-PPB. In non-neutral plasma electrons being near the center will possibly be in a similar situation. In the plasma electro-magnetic interactions must be introduced. It should be noted that in the case of a charged particle in a magnetic field the vortex quantization given by (9) can be read as

$$\begin{aligned} m\Gamma &= \oint_c (\nabla S - q\mathbf{A}) \cdot d\mathbf{s} \\ &= \oint_c \mathbf{p} \cdot d\mathbf{s} - q\Phi, \end{aligned} \quad (28)$$

where q is the charge of the particle and Φ is the magnetic flux passing through the enclosed surface. Analyzing vortex phenomena of non-neutral plasma in terms of the eigenfunctions of the 2D-PPB will be an interesting application.

The infinite freedom arising from the infinite degeneracy of the zero-energy solutions should be noticed. Such a freedom has never appeared in the statistical mechanics describing thermal equilibrium. The freedom is different from that generating the usual entropy and then temperatures, because the freedom does not change real energy observed in experiments at all. A model of statistical mechanics for the new freedom has been proposed and some simple applications have been performed in the case of 1D-PBB [51-53]. The model is applicable to slowly changing phenomena in the time evolutions, because the PPB has only pure imaginary energy eigenvalues in the 1-dimension. In the present model of the 2-dimensions, however, we have the infinite degree of freedom arising from the zero-energy solutions that have no time evolution. The huge degeneracy of the zero-energy solutions can provide the huge variety in every energy eigenstates, which will be identified by the vortex patterns. In such a consideration the vortex patterns will be understood as the topological properties of flows. How this freedom should be counted in statistical mechanics is an important problem in future considerations.

Finally we would like to comment that even in thermal equilibrium the freedom of the zero-energy flows can be used freely. Furthermore the use of the zero-energy flows is very useful and economical from the viewpoint of energy consumption. For example it can be a very economical step for the transmission of information. The transmission by the use of the zero-energy flows having the huge variety enable us to transmit an enormous amount of information without any energy loss. Considering that the flows are stationary, they can also be a very useful step for making mechanisms to preserve such information, i.e., for memories in living beings. The huge variety of vortex patterns can possibly discriminate the enormous amount of information. The change of the preserved memories can easily be carried out by changing the vortex patterns by the insertion of some zero-energy (stationary) flows in the preserved ones (see the processes presented in the section 3-1). Furthermore, as shown in the section 3-2, in all the time-dependent processes induced by the insertion of the unstable flows with complex energy eigenvalues

the time-dependent flows always turn back to the stationary flows in the long time scales, and then the initial flow patterns are recovered. That is to say, the initial patterns are kept in all such time-dependent processes. This stability of the flow patterns seems to be a very interesting property for the interpretation of the stability of memories not only in their preservations but in their applications as well. The applications, of course, mean thinking processes. The flows will possibly be workable in the steps for thinking in living beings. The use of the zero-energy and complex-energy solutions enables living beings to make up many functions in their bodies very economically on the basis of energy consumption. Anyway the zero-energy and complex-energy solutions are interesting objects to describe mechanisms working very economically as for the energy consumption. Especially, in the 2D-PPB case we can do it without any energy loss, because all the solutions of PPB have no real energy eigenvalue, i.e., the energy eigenvalues are zero or pure imaginary. Here we would like to summarize the property of flows in CSGT. As for the zero-energy flows we should stress the following three properties; (i) the absolutely energy-saving mechanism, (ii) the mechanism including an enormous topological variety, and (iii) the perfect recovery of the flow patterns in any disturbance by the insertions of arbitrary decaying flows with complex-energy eigenvalues. On the other hand the role of the flows with complex energies can be understood as the excitement mechanism among the zero-energy flows. We still have a lot of problems to overcome the present situation, but we may expect that the study of the zero- and complex-energy solutions in CSGT will open a new site in physics.

References

- [1] G. Blatter *et al.*, Rev. Mod. Phys. **66**, 1125 (1994).
- [2] G. W. Crabtree and D. R. Nelson, Phys. Today **50**, No.4 38 (1997).
- [3] R. E. Prange and M. Girvin M, *The Quantum Hall Effect* (Springer, New york, 1990), 2nd ed.
- [4] F. Wilczek, *Fractional Statistics and Anyon Superconductivity* (World Scientific, Singapore, 1990).
- [5] T. Chakaraborty and P. Pietiläinen, *The Quantum Hall Effects: Fractional and Integral* (Springer, New York, 1995), 2nd and updated ed.
- [6] S. Das Sarma and A. Pinczuk, A eds 1997 *Perspectives in Quantum Hall Effects* (Wiley, New York, 1997).
- [7] A. Khare, *Fractional Statistics and Quantum Theory* (World Scientific, Singapore, 1997).
- [8] K. S. Fine *et al.*, Phys. Rev. Lett. **75**, 3277 (1995).

- [9] Y. Kiwamoto *et al.*, J. Phys. Soc. Jpn. (Lett.) **68**, 3766 (1999).
- [10] Y. Kiwamoto *et al.*, Phys. Rev. Lett. **85**, 3173 (2000).
- [11] K. Ito *et al.*, Jpn. J. Appl. Phys. **40A**, 2558 (2001).
- [12] M. R. Matthews *et al.*, Phys. Rev. Lett. **83**, 2498 (1999).
- [13] C. Raman *et al.*, Phys. Rev. Lett. **83**, 2502 (1999).
- [14] K. W. Madison *et al.*, Phys. Rev. Lett. **84**, 806 (2000).
- [15] O. M. Marago *et al.*, Phys. Rev. Lett. **84**, 2056 (2000).
- [16] R. Fitzgerald *et al.*, Phys. Today **55**, No.8 19 (2000).
- [17] H. Lamb, *Hydrodynamics* (Cambridge Univ. Press, Cambridge, 1932), 6th ed.
- [18] L. D. Landau and E. M. Lifshitz, *Fluid Mechanics* (Pergamon, Oxford, 1987), 2nd ed.
- [19] G. K. Batchelor, *An Introduction to Fluid Dynamics* (Cambridge Univ. Press, Cambridge, 1967).
- [20] T. Tatsumi, *Hydrodynamics* (in Japanese) (Tokyo: Baihuukann 1982).
- [21] P. G. Saffman, *Vortex Dynamics* (Cambridge Univ. Press, Cambridge, 1992).
- [22] E. Madelung, Z. Phys. **40**, 322 (1926).
- [23] E. H. Kennard, Phys. Rev. **31**, 876 (1928).
- [24] L. de Broglie, *Introduction à l'étude de la Mécanique ondulatoire* (Hermann, Paris, 1930).
- [25] P. A. M. Dirac, Proc. R. Soc. London, Ser. A **209**, 291 (1951); *ibid.* **212**, 330 (1952); *ibid.* **223**, 438 (1954).
- [26] D. Bohm, Phys. Rev. **85**, 166, 180 (1952); *ibid.* **89**, 458 (1953).
- [27] T. Takabayasi, Prog. Theor. Phys. **8**, 143 (1952); *ibid.* **9**, 187 (1953).
- [28] M. Schönberg, Nuovo Cimento Soc. Ital. Fis., **12**, 103 (1954).
- [29] D. Bohm and J. P. Vigier, Phys. Rev. **96**, 208 (1954); *ibid.* **109**, 1882 (1958).
- [30] J. O. Hirschfelder, A. C. Christoph and W. E. Palke, J. Chem. Phys. **61**, 5435 (1974).
- [31] J. O. Hirschfelder, C. J. Goebel and L. W. Bruch, J. Chem. Phys. **61**, 5456 (1974).

- [32] J. O. Hirschfelder and K. T. Tang, J. Chem. Phys. **64**, 760; *ibid.* **65**, 470 (1976).
- [33] J. O. Hirschfelder, J. Chem. Phys. **67**, 5477 (1977).
- [34] S. K. Ghosh and B. M. Deb, Phys. Rep. **92**, 1 (1982).
- [35] H. Wu and D. W. L. Sprung, *Phys. Letters A* **183**, 413 (1993).
- [36] D. A. Schecter and H. E. Dubin, *Phys. Rev. Lett.* **83**, 2191 (1999).
- [37] I. Bialynicki-Birula, Z. Bialynicka-Birula and Śliwa C, *Phys. Rev.* **A61**, 032110 (2000).
- [38] T. Kobayashi, *Physica* **A303** (2002) 469 .
- [39] T. Kobayashi and T. Shimbori, *Phys. Rev.* **A65**, 042108 (2002).
- [40] A. Bohm and M. Gadella, *Dirac Kets, Gamow Vectors and Gel'fand Triplets* (Lecture Notes in Physics, Vol. 348, Springer, 1989).
- [41] T. Shimbori and T. Kobayashi, *J. Phys.* **A33**, 7637 (2000).
- [42] G. Barton, Ann. Phys. (N.Y.) **166**, 322 (1986).
- [43] P. Briet, J. M. Combes and P. Duclos, Commun. Partial Diff. Eqns. **12**, 201 (1987).
- [44] N. L. Balazs and A. Voros, Ann. Phys. (N.Y.) **199**, 123 (1990).
- [45] M. Castagnino, R. Diener, L. Lara and G. Puccini, Int. J. Theor. Phys. **36**, 2349 (1997).
- [46] T. Shimbori and T. Kobayashi, Nuovo Cimento Soc. Ital. Fis., B **115**, 325 (2000).
- [47] T. Shimbori, Phys. Lett. A **273**, 37 (2000).
- [48] M. S. Child, Proc. Roy. Soc. (London) **A292** (1966) 272.
- [49] M. S. Child, Mol. Phys. **12** (1967) 401.
- [50] J. N. L. Connor, Mol. Phys. **15** (1968) 37.
- [51] T. Kobayashi and T. Shimbori, Statistical mechanics for states with complex eigenvalues and quasi-stable semiclassical systems *Preprint cond-mat/0005237* (2000).
- [52] T. Kobayashi and T. Shimbori, *Phys. Lett.* **A280**, 23 (2001).
- [53] T. Kobayashi and T. Shimbori, *Phys. Rev.* **E63**, 056101 (2001).

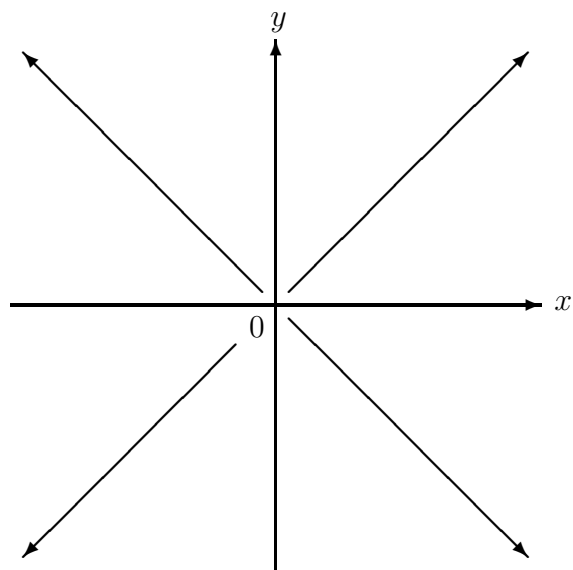


FIG. 1: Diverging flows.

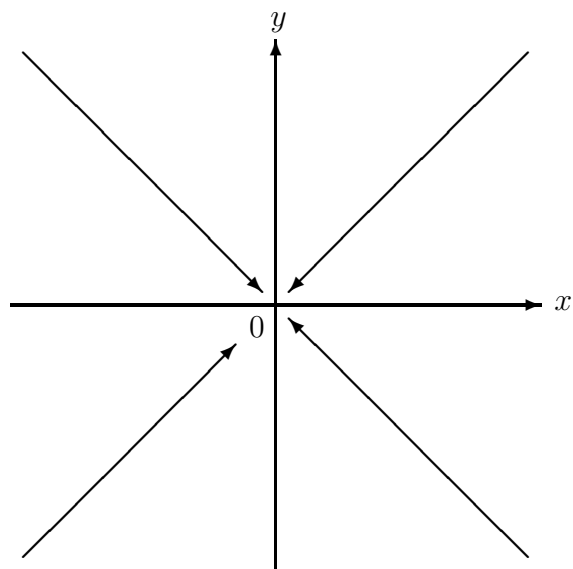


FIG. 2: Converging flows.

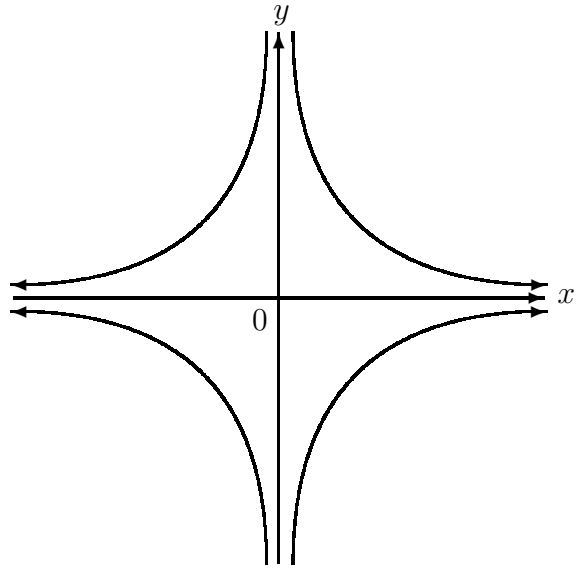


FIG. 3: Corner flows moving from the y -direction to the x -direction.

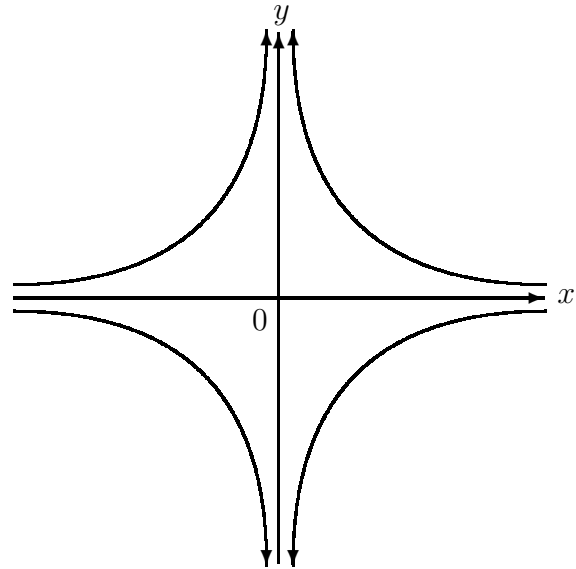


FIG. 4: Corner flows moving from the x -direction to the y -direction.

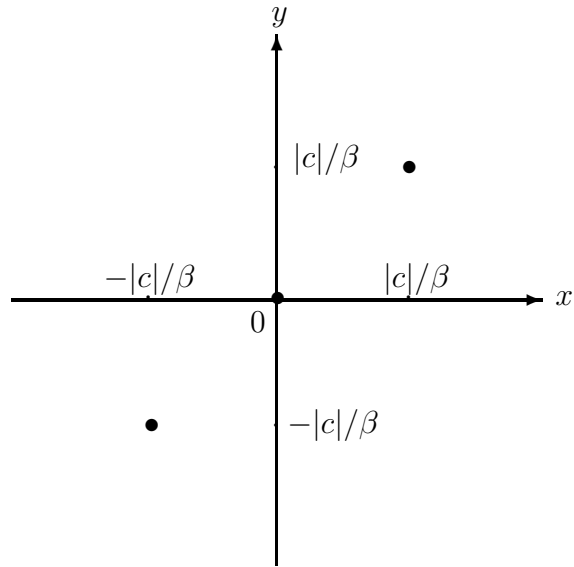


FIG. 5: Stationary pattern with three vortices. • denotes a vortex.

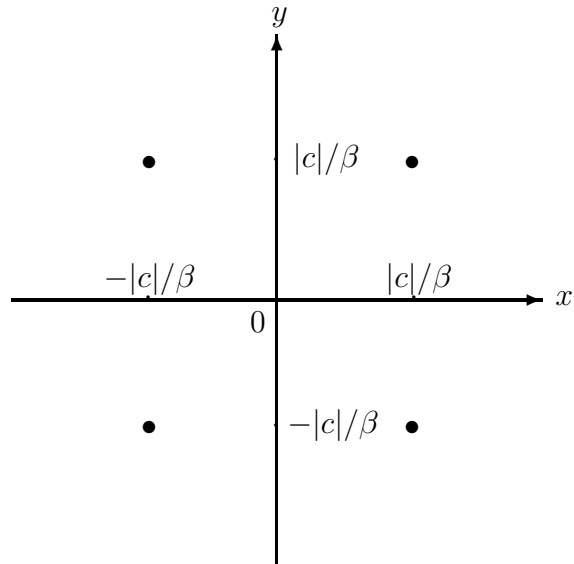


FIG. 6: Stationary pattern with four vortices.

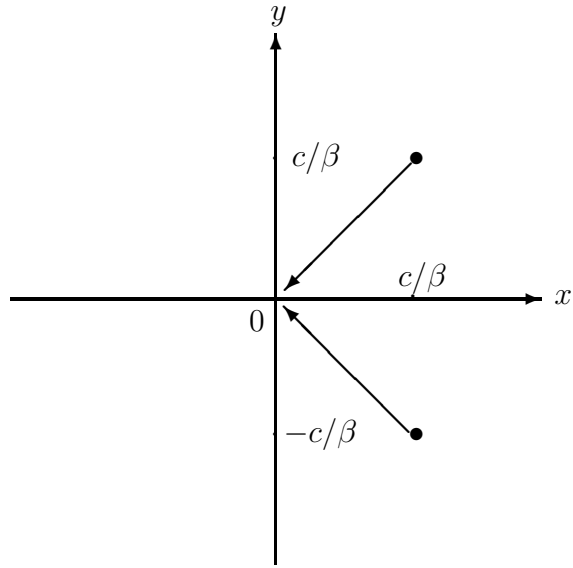


FIG. 7: A pair annihilation pattern for $c > 0$. The arrows show the moving directions of the vortices.

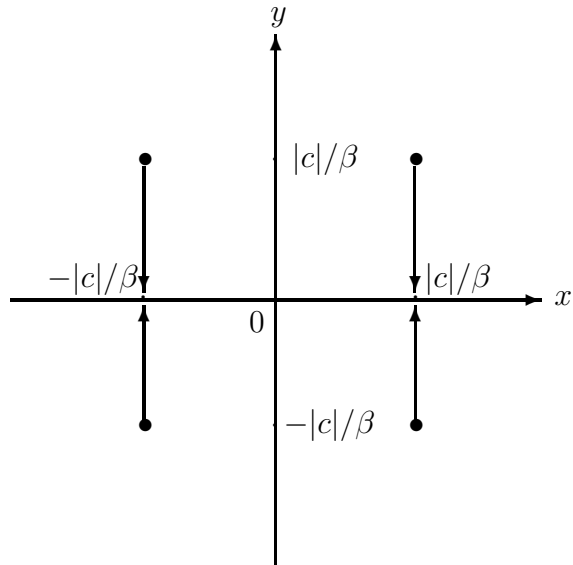


FIG. 8: Two pairs annihilation pattern.

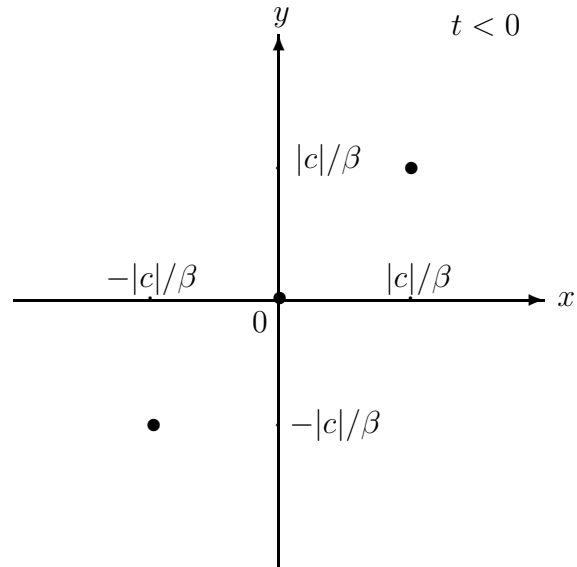


FIG. 9: Initial vortex pattern for $t < 0$.

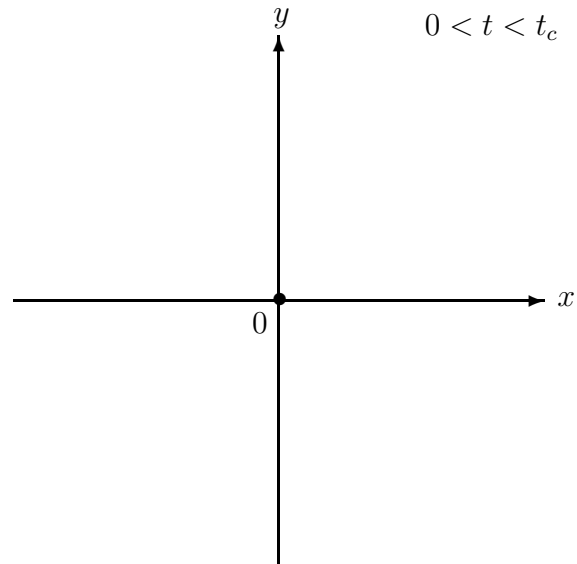


FIG. 10: Pattern with one vortex for $0 < t < t_c$.

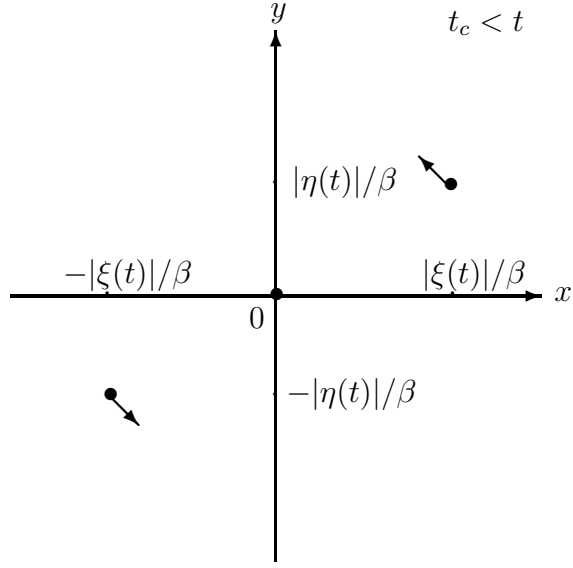


FIG. 11: Pattern with two moving vortices for $t_c < t$ in the case of $a > 0$.

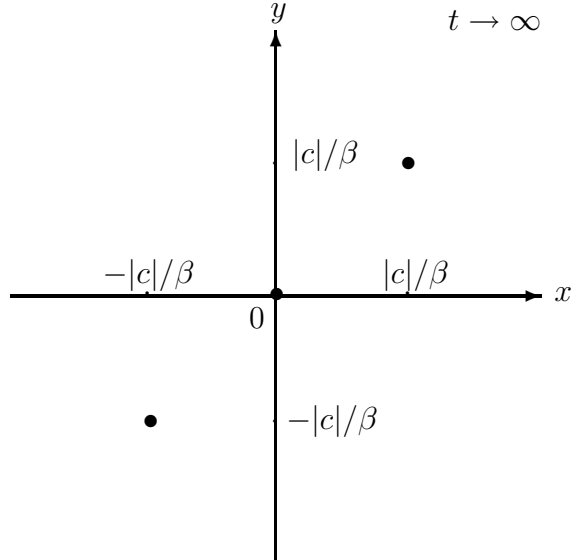


FIG. 12: Recovery of the initial vortex pattern in the limit $t \rightarrow \infty$.

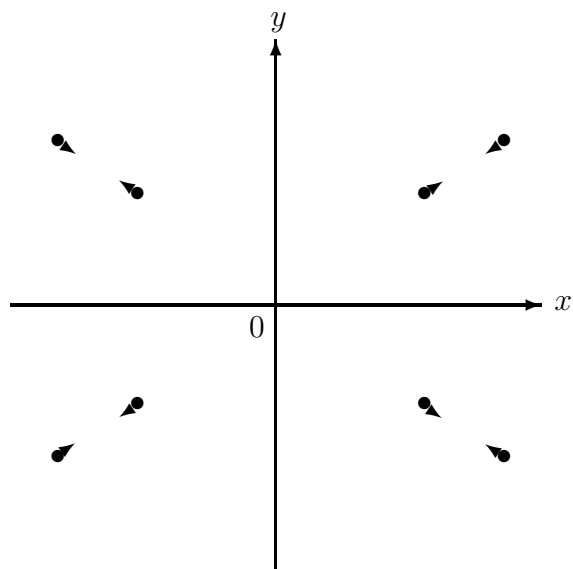


FIG. 13: Four pairs creation and annihilation.